ELSEVIER

Journal of Organometallic Chemistry 508 (1996) 169–181

Journal of Organometallic Chemistry

Ring slippage in indenyl derivatives of molybdenum and tungsten

José R. Ascenso [b], Isabel S. Gonçalves [a], Eberhardt Herdtweck [c], Carlos C. Romão [a,*]

[a] *Instituto de Tecnologia Química e Biológica, R. da Quinta Grande 6, 2780 Oeiras, Portugal*
[b] *Centro de Química Estrutural, Instituto Superior Técnico, 1096 Lisboa Codex, Portugal*
[c] *Anorganisch-chemisches Institut, Technische Universität München, D-85478 Garching, Germany*

Received 25 May 1995

Abstract

Ring slippage of the indenyl occurs upon dissolution of the complexes $[\eta^5\text{-IndM(CO)}_2\text{L}_2]\text{BF}_4$ (M = Mo or W; L = NCMe or dimethylformamide) in an excess of L, to give $[(\eta^3\text{-Ind})\text{M(CO)}_2\text{L}_3]\text{BF}_4$. Other ring-slipped complexes synthesized are $[(\eta^3\text{-Ind})\text{Mo(CO)}_2\text{L}_3]\text{BF}_4$ (L_3 = HC(pz)_3, $[\text{HB(pz)}_3]^-$, Me_3tacn or {en(NCMe)}). Addition of NCMe or an excess of L failed to give ring slippage in $[\eta^5\text{-IndMo(CO)}_2\text{L}_2]\text{BF}_4$ (L_2 = bipy, dppe, $(\text{PMe}_3)_2$, $\{\text{P(OMe)}_3\}_2$ or triphos). NMR and X-ray studies reveal a large folding of the η^3-indenyl ring.

The structure complex $[(\eta^3\text{-Ind})\text{W(CO)}_2(\text{NCMe})_3]\text{BF}_4$ (**5**) was determined by X-ray analysis.

Keywords: Molybdenum; Tungsten; Indenyl complexes; Ring slippage; X-ray structure

1. Introduction

The attempt to achieve better control of the reactivity of transition-metal organometallic complexes has raised the interest in indenyl as a substitute for cyclopentadienyl. In fact, the higher rates of substitution reactions of complexes of indenyl when compared with their cyclopentadienyl congeners has long been recognized under the name of "indenyl effect" [1]. The accepted interpretation of this kinetic effect rests on the easy "ring slippage" of the indenyl from η^5 to η^3 coordination. As the electron count at the metal is reduced by this ring slippage, associative pathways for substitution reactions are favoured. However, under certain conditions, the intermediate trihapto-complexes may be stable enough to be isolated and fully characterized. Hence reaction of a two-electron donor L′ with a coordinatively saturated cation $[(\eta^5\text{-Ind})\text{M(CO)}_2\text{-L}_2]^+$ (M = Mo (**1**) or W (**2**)) may lead either to addition or to substitution, as exemplified by Eq. (1). In principle, the outcome of the reaction will depend on the stability of the trihapto complex which, in turn, will depend on the nature and number of the ancilliary ligands L. Substitution is the general result and, surprisingly, additions accompanied by $\eta^5 \rightarrow \eta^3$ "ring slippage" are relatively rare in spite of the many known examples of coordinatively saturated complexes with η^3-indenyl [2].

The first thoroughly characterized example was reported by Merola et al. [3] in 1986:

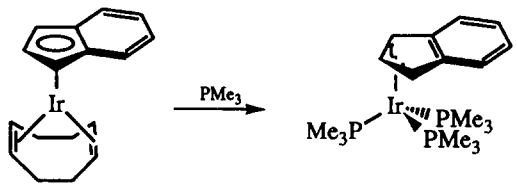

(2)

It follows the reports on the less expected $\eta^5 \rightarrow \eta^1$ ring slippages established earlier by Casey and O'Connor [4]

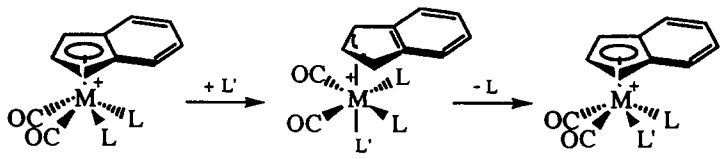

(1)

* Corresponding author.

Elsevier Science S.A.
SSDI 0022-328X(95)05859-1

in which all attempts to intercept the intermediate η^3-indenyl complex were unsuccessful:

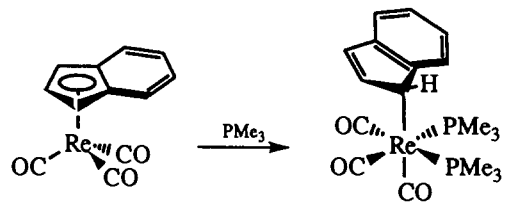

(3)

We have previously observed a facile ring slippage of the indenyl ligand in a tungsten complex by ^{1}H NMR spectroscopy as described by [5]

$$[(\eta^5\text{-Ind})W(NCMe)_2(CO)_2]BF_4 \underset{CH_2Cl_2}{\overset{NCMe}{\rightleftharpoons}} [(\eta^3\text{-Ind})W(NCMe)_3(CO)_2]BF_4 \quad (4)$$

The present study reports the structural characterization of $[(\eta^3\text{-Ind})W(CO)_2(NCMe)_3]BF_4$ as well as describing a number of additions to the 18-electron cations $[(\eta^5\text{-Ind})M(CO)_2L_2]^+$ (M = Mo or W) in order to ascertain the conditions most favourable for "ring slippage".

2. Results and discussion

2.1. Chemical studies

The coordinatively saturated cations used in this work, $[(\eta^5\text{-Ind})M(CO)_2L_2]^+$ (M = Mo (**1**) or W (**2**)) are prepared as depicted in Scheme 1. The starting complexes $[(\eta^5\text{-Ind})M(\eta^3\text{-}C_3H_5)(CO)_2]$ (M = Mo or W) [6] are protonated with $HBF_4 \cdot OEt_2$, in CH_2Cl_2 at room temperature, and the resulting red solution treated with the desired L to give the products **1a–1i** (M = Mo) and **2**(M = W) with good isolated yields. This method has already been used by Cutler and coworkers [7] to prepare some cyclopentadienyl analogues $[CpMo(CO)_2L_2]BF_4$ and by us [5,6] to prepare a wide range of cyclopentadienyl and indenyl complexes with dienes, of general formula $[Cp'M(CO)_2(diene)]BF_4$ (Cp' = Cp, MeCp or Ind). The products are listed in Table 1, together with some selected ^{1}H NMR data. Compounds **1a**, **1f** and **1h** are known but have been prepared by a different method [8a]. The acetonitrile derivative has been described in the literature as a useful promoter of diene transformations [8b,9].

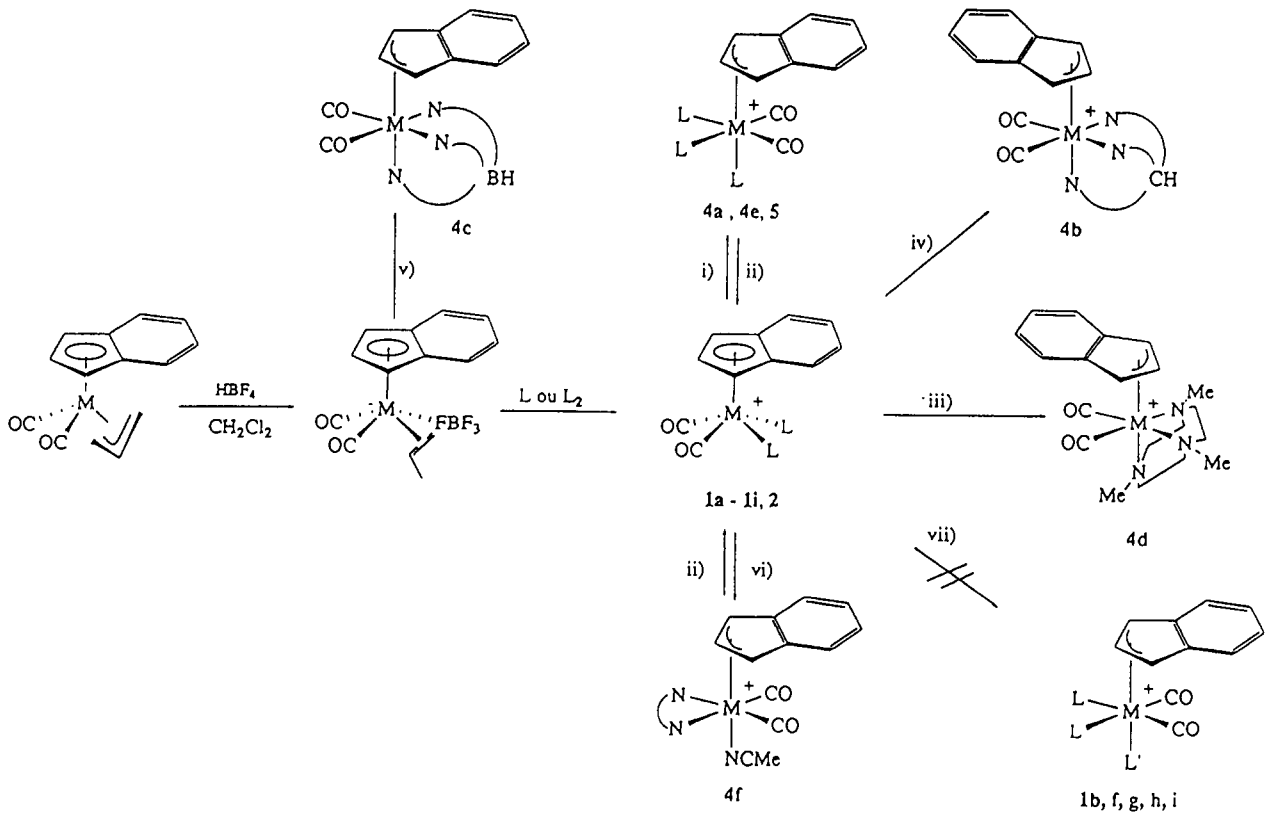

Scheme 1. (i) **1a**, **2** in NCMe or **1d** in dimethylformamide (DMF), at room temperature; (ii) **4a**, **4e** and **4f** in CH_2Cl_2; (iii) Me_3tacn in CH_2Cl_2; (iv) **1c** dissolved in NCMe at 45°C; (v) $KHB(pz)_3$ in CH_2Cl_2; (vi) **1e** in NCMe, L_2 = en; (vii) **1b**, **1f**, **1g**, **1h** and **1i** with an excess of L or NCMe at reflux.

Table 1
List of $[(\eta^5\text{-Ind})M(CO)_2L_2]BF_4$ compounds prepared and selected ^1H NMR

Compound	Ligand L_2	η^5-indenyl resonances (room temperature), δ (ppm)		
		$H^{5/8}$	$H^{1/3}$	H^2
Mo				
1a	$(NCMe)_2$	7.60–7.54 m	6.07 d	5.02 t
1b	bipy	6.95 m; 6.66 m	6.47 d	5.47 t
1c	tpm	–	–	–
1d	$(DMF)_2$	7.47 m; 7.39 m	6.15 d	4.98 t
1e	en	7.84 m; 7.51 m	6.23 d	5.18 t
1f	$(P(OMe)_3)_2$	7.59 m; 7.30 m	6.07 d	5.60 t
1g	$(PMe_3)_2$	7.66 m; 7.28 m	5.85 d	5.54 t
1h	dppe	7.08 m; 6.01 m	5.59 d	5.28 t
1i	triphos	7.06 m; 6.58 m	5.36 d	5.71 t
W				
2	$(NCMe)_2$	7.52 s	6.16 d	5.24 t

pz = pyrazolyl, tpm = trispyrazolylmethane, dppe = 1,2-bis-(diphenylphosphino)ethane.
en = ethylenediamine; DMF = *N*,*N*-dimethylformamide, triphos = 1,1,1-tris(diphenylphosphinomethyl)ethane
The numbering scheme is as follows:

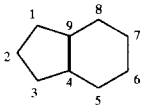

The characterization of most complexes in Table 1 is straightforward. The presence of a *cis*-$M(CO)_2$ unit is clear from the observed IR data which show, in all cases, two bands in the $\nu(CO)$ region. These values are, of course, dependent on the nature of L, they are higher for $P(OMe)_3$ and dppe but relatively invariant for all the other ligands.

All the ^1H NMR spectra show a similar pattern for the resonances of the η^5-indenyl, two sets of signals for the C_6 ring protons (H^{5-8}) at $\delta \approx 7.70$ and 7.30 ppm, a doublet at $\delta \approx 6.0$ ppm ($H^{1/3}$) and a triplet between $\delta \approx 5.00$ and 5.60 ppm (H^2) (see Table 1 for the numbering scheme). The exceptions are the H^{5-8} resonances of the bipy, dppe and triphos complexes which are shifted to higher field by about 0.5 ppm. This pattern and chemical shift values are observed, for example, in the mixed-ring metallocene derivatives $[(\eta^5\text{-ind})(\eta^5\text{-Cp})ML_2]^{n+}$ [5,6]. The bidentate coordination of tris(pyrazolyl)methane in **1c** can only be assumed on the basis of several analogies. In fact, unlike

Table 2
Selected ^1H and ^{13}C NMR data of $[(\eta^3\text{-Ind})M(CO)_2L_3]BF_4$ and some related complexes

Compound	Ligand L_3	^1H and ^{13}C η3-indenyl resonances, δ (ppm) [a]			
		H^2	$H^{5/8}$	$H^{1/3}$	C^4/C^9
Mo					
4a	$(NCMe_3)$ [b]	7.20 t	6.47–6.37 m	5.10 d	146.73
4b	tpm	6.90 t	6.70 m; 6.55 m	5.55 d	147.80
4c	tpb	6.63 t	6.68 m; 6.50 m	5.40 d	148.56
4d	Me_3tacn	6.94 t	6.60 m; 6.47 m	4.78 d	147.03
4e	$(DMF)_3$ [c]	6.99 t	6.47 m; 6.39 m	5.08 d	146.73
4f	(en)(NCMe)	7.07 t	6.48 m; 6.41 m	5.10 d	–
	η^5-Cp [d]	6.75 t	6.67 m; 6.43 m	5.20	151.10
W					
5	$(NCMe)_3$	6.46 t	6.55–6.42 m	5.02 d	149.23
	η^5-Cp [e]	7.07 t	6.66–6.47 m	4.95 d	152.03
	η^5-Ind [f]	3.4	6.6 m	4.8	–

[a] All spectra in CD_3CN at room temperature except otherwise indicated: see Table 1 for numbering.
[b] In CD_3CN at -45°C.
[c] In DMF.
[d] Ref. [6].
[e] [5].
[f] [12]; tpb = hydrotrispyrazolylborato; Me_3tacn = 1,4,7-*N*,*N*′,*N*″-trimethyltriazacyclononane.

all the other $[(\eta^5\text{-Ind})M(CO)_2L_2]BF_4$ cations reported here, **1c** precipitates instantaneously from the reaction mixture and its insolubility precludes NMR studies. The IR spectrum has two CO stretching vibrations at values rather similar to those of other similar η^5-indenyl complexes, such as **1a**, **1b** and **1g**, as expected on bidentate coordination of $HC(pz)_3$ (cf. **4b** below). Furthermore, this spectrum is very similar to that of $[CpMo\{\eta^2\text{-}HC(pz)_3\}(CO)_2]BF_4$ (**3**) which is readily prepared from $[CpMo(\eta^3\text{-}C_3H_5)(CO)_2]$ after protonation and reaction

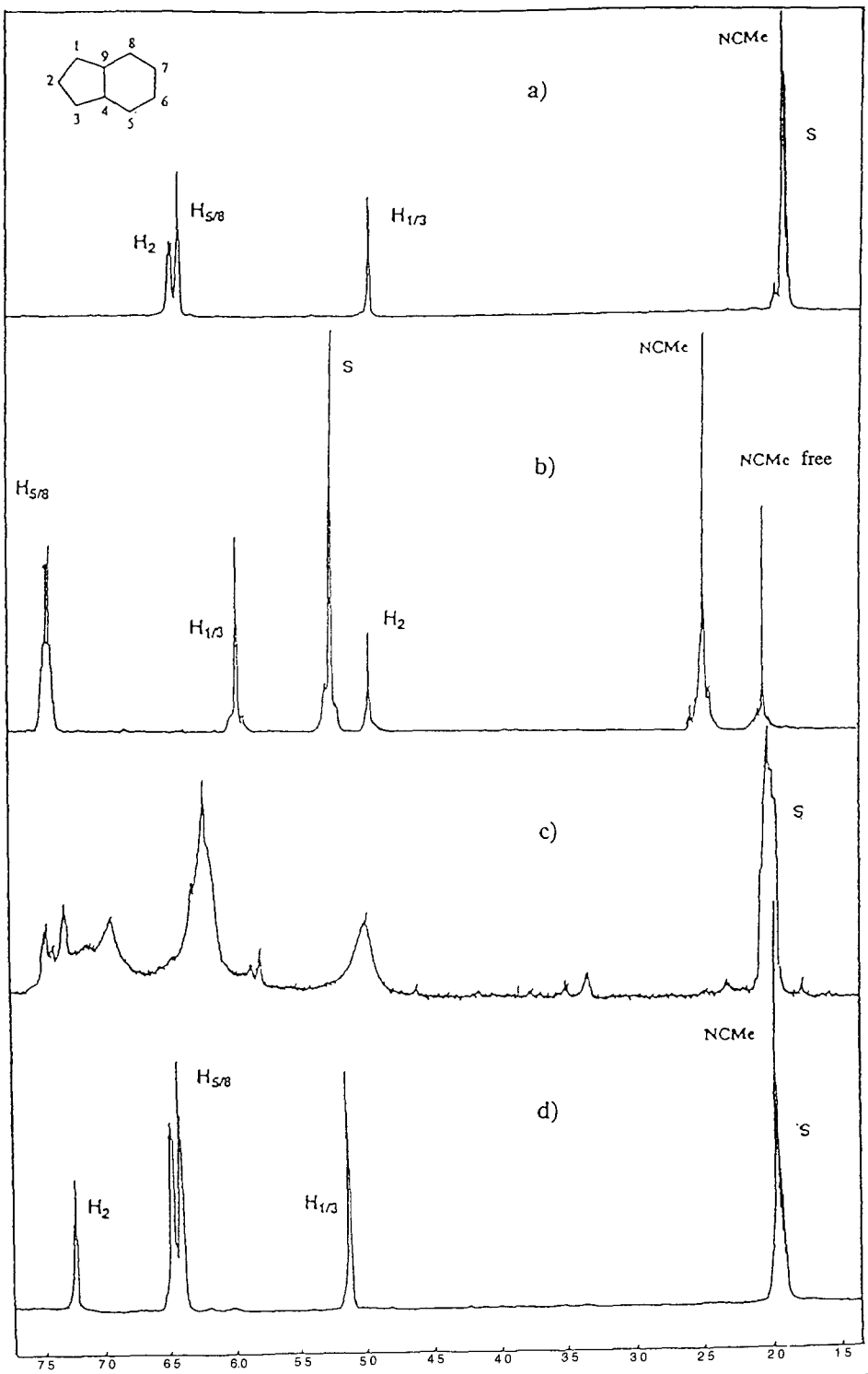

Fig. 1. ^1H NMR spectra (300 MHz) showing δ (ppm) of the complexes (S = solvent) (a) $[IndW(CO)_2(NCMe)_3]BF_4$ in NCMe (room temperature), (b) $[IndMo(CO)_2(NCMe)_3]BF_4$ in CD_2Cl_2, (c) $[IndMo(CO)_2(NCMe)_3]BF_4$ in NCMe (room temperature) and (d) $[IndMo(CO)_2(NCMe)_3]BF_4$ in NCMe (40°C).

with $HC(pz)_3$. Consistent with a bidentate coordination of $HC(pz)_3$, the ^1H NMR spectrum of **3** has two sets of pyrazolyl signals with relative intensities of 2.1, one of which appears at higher field and corresponds to the dangling pyrozolyl [10]. The insolubility of **1c** is paralleled in other $HC(pz)_3$ complexes, such as $[Mo\{HC(pz)_3\}(CO)_3]$ [11] and has been attributed to oligomerization or polymerization by means of M–pz–C–pz-M bridges. A similar situation is observed in **1i** where the triphos is bidentate with a dangling arm, as shown by ^1H NMR spectroscopy.

When **1a** or **2** are dissolved in NCMe, the colour darkens markedly. Addition of ether to the resulting solutions allows the isolation of crystalline $[(\eta^3\text{-Ind})M(CO)_2(NCMe)_3]BF_4$ (M = Mo (purple) (4a) or W (ruby-red) (**5**)). This change is faster when the solutions are at about 40°C. At room temperature, the ^1H NMR spectrum of **4a**, in NCMe-d_3, shows rather broad peaks, suggesting extensive dynamic structural interconversions (Fig. 1(c)). Upon cooling to −40°C the spectrum of **4a** becomes well resolved and sharp resonances are observed (Fig. 1(d)). Such a dynamic behaviour is absent in the spectrum of **1a** in CD_2Cl_2, which is sharp at room temperature (Fig. 1(b)). In fact, the ^1H NMR spectrum of **4a** in CD_2Cl_2 (Fig. 1(b)) corresponds to the spectrum of **1a** and 1 equivalent of free NCMe.

The pattern of the resonances for both **4a** at −40°C and **5** at room temperature, is best interpreted on the basis of the trihapto coordination of the indenyl. With regard to the Mo complexes, an upfield shift (about 1.1 ppm) of the benzenoid protons (H^{5-8}) and a remarkable downfield shift (about 2.2 ppm) of the *meso*-pseudoallylic H^2 signal are the most significant differences between **1a** and **4a** (Table 2).

Similar but slightly smaller variations in chemical shifts are observed for the pair of analogous W complexes **2** and **5**. These values are within the range of those measured in the trihapto-indenyl complexes $[(\eta^3\text{-Ind})CpM(CO)_2]$ (M = Mo or W) [5,6] (see also Table 2) and these reported for $[(\eta^3\text{-Ind})Ir(PMe_3)_3]$: δ = 7.09(H^2), 6.55 (H^{5-8}) ppm [3]. In contrast with this pattern, the value of the chemical shift of H^2 observed

Table 3
Selected bond distances (pm) and angles (°) for $[\eta^3\text{-IndW}(CO)_2(NCMe)_3]BF_4$ (**5**), where Cm(1) denotes the centre of gravity in C(6), C(7) and C(7)a, and Cm(2) denotes the centre of gravity in C(16), C(17) and C(17)a

Molecule **A**		Molecule **B**	
Bond distances			
W(1)–N(1)	215.3(7)	W(2)–N(3)	215.8(7)
W(1)–N(2)	219.5(5)	W(2)–N(4)	219.0(5)
W(1)–C(1)	196.6(5)	W(2)–C(11)	197.1(5)
W(1)–C(6)	215.7(8)	W(2)–C(16)	218.5(8)
W(1)–C(7)	239.3(6)	W(2)–C(17)	236.9(6)
W(1)–Cm(1)	208.1	W(2)–Cm(2)	207.7
O(1)–C(1)	115.7(7)	O(2)–C(11)	115.0(7)
N(1)–C(2)	113.9(10)	N(3)–C(12)	111.7(10)
N(2)–C(4)	113.3(8)	N(4)–C(14)	112.2(10)
C(2)–C(3)	147.1(13)	C(12)–C(13)	144.1(15)
C(4)–C(5)	143.8(10)	C(14)–C(15)	146.6(15)
C(6)–C(7)	143.2(8)	C(16)–C(17)	141.9(8)
C(7)–C(8)	147.0(7)	C(17)–C(18)	148.1(7)
C(8)–C(9)	137.8(7)	C(18)–C(19)	138.0(7)
C(8)–C(8)a	142.0(6)	C(18)–C(18)a	141.6(7)
C(9)–C(10)	140.9(8)	C(19)–C(20)	140.6(9)
C(10)–C(10)a	135.9(10)	C(20)–C(20)a	137.2(10)
Bond angles			
N(1)–W(1)–N(2)	80.6(2)	N(3)–W(2)–N(4)	80.8(2)
N(1)–W(1)–C(1)	90.5(2)	N(3)–W(2)–C(11)	90.3(2)
N(2)–W(1)–C(1)	96.7(2)	N(4)–W(2)–C(11)	96.8(2)
N(2)–W(1)–N(2)a	83.3(2)	N(4)–W(2)–N(4)a	83.4(2)
N(2)–W(1)–C(1)a	171.0(2)	N(4)–W(2)–C(11)a	170.9(2)
C(1)–W(1)–C(1)a	81.9(2)	C(11)–W(2)–C(11)a	81.6(2)
N(1)–W(1)–Cm(1)	172.8	N(3)–W(2)–Cm(2)	173.3
N(2)–W(1)–Cm(1)	94.1	N(4)–W(2)–Cm(2)	94.2
C(1)–W(1)–Cm(1)	94.9	C(11)–W(2)–Cm(2)	94.8
W(1)–N(1)–C(2)	176.7(6)	W(2)–N(3)–C(12)	176.5(6)
W(1)–N(2)–C(4)	176.1(5)	W(2)–N(4)–C(14)	178.2(6)
W(1)–C(1)–O(1)	176.0(5)	W(2)–C(11)–O(2)	177.2(5)
N(1)–C(2)–C(3)	179.5(9)	N(3)–C(12)–C(13)	180.0(6)
N(2)–C(4)–C(5)	178.8(7)	N(4)–C(14)–C(15)	178.6(9)

in [(η^5-Ind)M(η^3-Ind)$(CO)_2$] is abnormally low (Table 2). This exceptional situation is most certainly due to the influence of the ring current of the benzenoid ring of the ancilliary indenyl.

The values of the ν(CO) stretching vibrations change little in each of the transformations **1a** → **4a** ν(CO)(KBr), 1959, 1871 → 1964, 1869 cm^{-1}; ν(CO) (Nujol), 1979, 1888 → 1962, 1890 cm^{-1} and **2** → **5** (ν(CO)(KBr), 1955, 1879 → 1948, 1874 cm^{-1}; ν(CO) (Nujol), 1954, 1879 → 1952, 1881 cm^{-1}).

Further confirmation of the trihapto coordination of the indenyl ring in **4a** and **5** stems from the large downfield shift (deshielding) of the ring junction C^4 and C^9 carbon atoms in the ^{13}C NMR spectra (see Table 2). These types of values also indicate that the η^3-indenyl in **4a** and **5** is associated with a marked slip-fold distortion. Values of $\delta \approx 120$ ppm for these quaternary carbon atoms correspond to a typical η^5-indenyl with a fold angle (Ω; see [13] for definition) close to 0°, i.e. planar. An appreciable degree of bending, $\Omega = 8.5°$, has already been found for $\delta \approx 127$ ppm [14b]. Strongly bent rings have C^4 and C^9 resonances at higher δ values as exemplified for [(η^3-Ind)Ir$(PMe_3)_3$] ($\Omega = 28°$; $\delta = 156.7$ ppm; C^4–C^9) [3] and [CpMo(η^3-Ind)$(CO)_2$] ($\Omega = 26°$; $\delta = 151.1$ ppm; C^4–C^9) [6a]. In the present case, the values of $\delta = 146.73$ and 149.23 ppm for **4a** and **5** imply a large Ω, about 20°. A crystal structure determination of **5** confirms these assignments. The crystals of **5** are built up of discrete monomeric ions. Two crystallographically independent cations and anions are located on a mirror plane. The BF_4^- anions are disordered on two equivalently occupied positions. Both cations (molecule **A** and molecule **B**) are identical in their three-dimensional assemblies within standards limits. Therefore only **A** will be discussed. In **5A** the molecular structure is best described as a slightly distorted octahedron around the tungsten atom with two acetonitrile ligands together with two carbonyl groups in the equatorial plane. The two remaining apices are occupied by an additional acetonitrile molecule and the indenyl group. A view of the molecule is shown in Fig. 2 with the appropriate numbering scheme. Relevant bond angles and distances are given in Table 3.

The metal atom W(1) and one acetonitrile group N(1), C(2), C(3) are located on the mirror plane which bisects the indenyl through C(6). As expected from the NMR measurements, the indenyl is clearly η^3 coordinated. Using the slip parameters of Faller et al. [13], the W(1) atom has slipped a distance $|S| = 130.7$ pm (**B** $|S| = 127.7$ pm) (!) away from the centroid of the five-membered ring. A key feature is the folding of the uncomplexed "ene fragment" (C(8), C(8)a in Fig. 2) (these atoms are numbered C^4 and C^9 in the NMR discussion above) of the benzonoid part of the indenyl ligand. The observed fold angle Ω is 24.1° (**B**, $\Omega = 27.4°$). Table 4 compares all the slip parameters of **5** with those of other related and fully characterized η^3–η^5 indenyl complexes.

To the best of our knowledge, **5** is the first hexacoordinated tungsten complex with an indenyl at the apical

Table 4
Slip parameters (defined in [13,15]) for [η^3-Ind$W(CO)_2(NCMe)_3$]BF_4 (**5**) and related compounds

Compound	$\Delta = \|S\|$ (pm)	σ (°)	Ψ (°)	Δ(M–C) (pm)	Ω (°)	References
[Ind$W(CO)_2(NCMe)_3$]$^+$						This work
η^3-ind A	130.7	0.0	33.0	93.5	24.1	
η^3-ind B	127.7	0.0	32.3	91.3	27.4	
[$Ind_2V(CO)_2$]$^+$						[15]
η^5-ind 1	19.2	27.9	5.6	13	No	
η^5-ind 2	19.7	17.7	5.8	15	No	
[$Ind_2V(CO)_2$]						[16]
η^5-ind	15.7	0.0	4.6	13	No	
η^3-ind	79.8	1.5	20.9	56	12.0	
[$Cp_2W(CO)_2$]						[17]
η^5-Cp	7.6	0	2.2	10	4.9 [a]	
η^3-Cp	92.8	0	23.4	62	19.7	
[IndCpMo(NCME)]$^{2+}$						[6b]
η^5-Cp	6.5	9.7	1.9	4	No	
η^5-Ind	19.4	2.6	5.6	15	5.1	
[IndCpMo$(CO)_2$]						[6a]
η^5-Cp	12.0	0.6	3.4	9	2.1	
η^3-ind	94.7	6.0	24.1	65	21.4	

[a] Value may be incorrect.

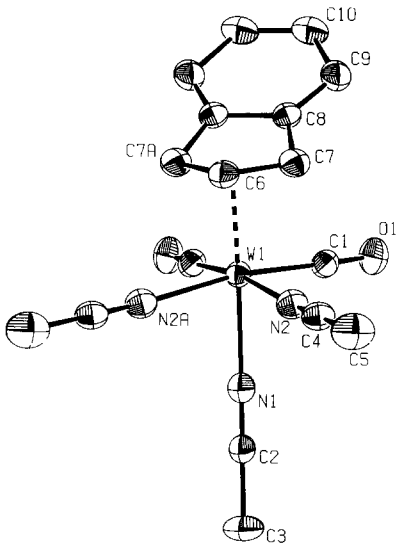

Fig. 2. Molecular structure of the cation **5** showing 50% probability ellipsoids and the atom-labelling scheme. Hydrogen atoms are omitted for clarity. A crystallographic mirror plane passes through C(3), C(2), N(1), W(1) and C(6). The operator for generating equivalent atoms is $(-x, y, z)$.

position, and up to now only three other similar tungsten η-allyl complexes have been structurally characterized: $[(\eta^3\text{-}C_3H_5)(CF_3COO)(CO)_2W(MeOCH_2CH_2OMe)]$ [19] $[(\eta^3\text{-}C_3H_5)Br(CO)_2W\text{-}(C_6H_{11}N{=}CH{-}CH{=}N\ C_6H_{11}\text{-}N,N')]$ [20] and $[N(Et)_4]\ [\eta^3\text{-}(C_3H_5)Cl_2(CO)_2WP(C_6H_5)_3]$ [21]. All interatomic distances and angles are within the expected values for a hexacoordinated tungsten atom and fit those published in [19–21]. The conformation relative to the carbonyls of the indenyl in **5** is the same as observed in these η-allyl complexes and schematically represented in **a**; the open side of the coordinated allyl (or pseudo allylic) atoms is oriented towards the quadrant defined by the carbonyls. In other words, the directions defined between the central and terminal allylic (or pseudo allylic) carbons are projected over the M–CO directions in an eclipsed fashion. This conformation seems to be rather general for $[L_3M(CO)_2(\eta^3\text{-allyl})]^{n+}$ species (M = Mo or W) and is also observed in the crystal structure of $[Mo(\eta^3\text{-}C_3H_5)(CO)_2(CH_3CN)(bipy)]^+$. Molecular orbital (MO) calculations on this complex **a** at the extended Hückel level show it to be preferred over the rotated conformer [22]. Conformation **b** is present in the isoelectronic $[CpMo(\eta^3\text{-Ind})(CO)_2]$.

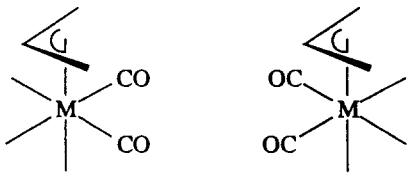

a **b**

As exemplified by the spectrum in Fig. 1(b) and later by product isolation, redissolution of **4a** and **5** in CH_2Cl_2 results in the expulsion of one coordinated NCMe and the inverse haptotropic shift, to form **1a** and **2** respectively Eq. (4) [5].

These mild reaction conditions show that ring slippage between **1a** and **4a** as well as between **2a** and **5** is very facile and prompted a study of similar reactions with other donors, which are also summarized in Scheme 1. Dissolution and recrystallization of the DMF complex $[(\eta^5\text{-Ind})Mo(CO)_2(DMF)_2]BF_4$ (**1d**) from DMF gives the ring-slipped adduct $[(\eta^3\text{-Ind})Mo(CO)_2(DMF)_3]BF_4$ (**4e**). In contrast with the structural flexibility of **4a** at room temperature, the ^1H NMR spectrum of **4e**, in DMF-d_7, is well resolved and compatible with the presence of a structurally rigid species **4e** with a well-defined η^3-Ind (H^2 at $\delta = 6.99$ ppm). This spectrum remains invariant at low temperatures showing that DMF is less labile than the NCMe in this systems. The low field chemical shifts of the C^4–C^9 junction atoms in the ^{13}C NMR spectrum suggests a high degree of folding. An intermediate behaviour is found for the ethylenediamine complex **1e**. At room temperature its ^1H NMR spectrum, NCMe-d_3, looks like that of **4a**, revealing dynamic interconversions. However, at −45°C, two species still remain clearly identifiable: **1e**, characterized by its H^2 at $\delta = 5.18$ ppm, and a trihapto-indenyl complex, $[(\eta^3\text{-Ind})Mo(CO)_2(en)(NCMe)]BF_4$ (**4f**), characterized by H^2 at $\delta = 7.07$ ppm. Under these circunstances, it is not surprising that **1c** readily rearranges, in warm acetonitrile, to give the ring-slipped complex $[(\eta^3\text{-Ind})Mo(CO)_2\{\eta^3\text{-}HC(pz)_3\}]BF_4$ (**4b**) in which the tpm becomes tridentate. The complex is now freely soluble in CH_2Cl_2 and the ^1H NMR and ^{13}C NMR spectra are consistent with this structural rearrangement. The *meso* H^2 of the indenyl appears at low field ($\delta = 6.90$ ppm), and the C^4–C^9 resonances at $\delta = 147.80$ ppm indicate a clearly folded η^3-indenyl. The two ν(CO) bands appear now at 1946 and 1867 cm^{-1} (Nujol mull) instead of 1958 and 1883 cm^{-1} (KBr pellet). This set of data is similar to that observed for the neutral hydrotrispyrazolylborate analogue $[(\eta^3\text{-Ind})Mo(CO)_2\{\eta^3\text{-}HB(pz)_3\}]$ (**4c**) obtained from the reaction of **1a** with $K[HB(pz)_3]$. Likewise, reaction of **1a** with the triaza-macrocycle Me_3tacn (Me_3tacn = 1,4,7-*N*,*N*′,*N*″-trimethyltriazacyclononane) gives the ring-slipped complex $[(\eta^3\text{-Ind})Mo(CO)_2\{\eta^3\text{-}Me_3tacn\}]$ (**4d**). In both cases, no signs of an intermediate such as $[(\eta^5\text{-Ind})Mo(CO)_2\{\eta^2\text{-}HB(pz)_3\}]$ were detected although we believe that the transformations of **1c** into **4b** as well as the formation of **4c** and **4d** proceed by stepwise $\eta^5 \rightarrow \eta^3$ haptotropic shifts from initially formed complexes $[(\eta^5\text{-Ind})M(CO)_2L_2]^+$ where the nitrogen ligands are bidentate ($L_2 = CH(pz)_3$, $[HB(pz)_3]^-$ or Me_3tacn).

Table 5
Three examples of $\eta^5 \rightarrow \eta^3$ ring slippages in indenyl complexes

η^5-Ind → η^3-Ind ring slippage reactions	Reference
$[(\eta^5\text{-Ind})\text{Ir(COD)}] + PMe_3$ (exc) → $[(\eta^3\text{-Ind})\text{Ir}(PMe_3)_2]$	[3]
$[(\eta^5\text{-Ind})\text{Fe}(CO)_2]^- + CO$ (1 atm) → $[(\eta^3\text{-Ind})\text{Fe}(CO)_3]^-$	[23]
$[(\eta^5\text{-Ind})_2\text{V}] + CO$ (1 atm) → $[(\eta^5\text{-Ind})(\eta^3\text{-Ind})\text{V}(CO)_2]$	[17]

Formally, **4b–4d** are analogues of $[Cp'Mo(\eta^3\text{-ind})(CO)_2]$ (Cp′ = Cp or Ind) reported elsewhere [5,6]. Complex **4d** is only accessible from the bis(acetonitrile) complex **1a** and not directly from species $[(\eta^5\text{-Ind})Mo(CO)_2(\eta^2\text{-}C_3H_6)FBF_3]$ as noted in Scheme 1. Nitrogen bases such as Me_3tacn, NEt_3 or even aniline deprotonate the propene, as shown [22] by

$$[(\eta^5\text{-Ind})Mo(\eta^3\text{-}C_3H_5)(CO)_2] \underset{Me_3tacn}{\overset{HBF_4}{\rightleftharpoons}} [(\eta^5\text{-Ind})Mo(\eta^2\text{-}C_3H_6)(CO)_2FBF_3] \quad (5)$$

Having gathered all this evidence about ring-slippage reactions in $[(\eta^5\text{-Ind})M(CO)_2L_2]^+$, we assumed that many other trihapto-indenyl complexes of general formula $[(\eta^3\text{-Ind})M(CO)_2L_2L']^+$ could be obtained by addition of L or L′ to the bipyridyl, phosphine or phosphite complexes **1b**, **1f–1i** according to

$$[(\eta^5\text{-Ind})M(CO)_2L_2]^+ + L' \longrightarrow [(\eta^3\text{-Ind})M(CO)_2L_2L']^+ \quad (6)$$

Very much to our surprise, none of the reactions tried led to the expected addition or ring-slippage processes. In fact, the bipy, dppe and triphos derivatives, **1b**, **1h** and **1i**, remain unchanged after 12 h in refluxing NCMe. Preparative as well as in-situ ^1H NMR experiments showed that the $P(OMe)_3$ and PMe_3 derivatives, **1f** and **1g**, also remain unchanged after prolonged reaction times (NCMe or CH_2Cl_2) in the presence of large excesses of $P(OMe)_3$ and PMe_3 respectively.

To the best of our knowledge, only three other examples of clear-cut $\eta^5 \rightarrow \eta^3$ ring slippages in indenyl complexes, promoted by donor addition, have been reported, as summarized in Table 5.

In the case of Ir-d_8, PMe_3 or PMe_2Ph is necessary for the ring slippage to take place and CO is ineffective. In contrast, the very electron-rich iron and vanadium complexes undergo this slippage in the presence of CO at 1 atm. In the case of the three-legged piano-stool d_6 complex $[IndRe(CO)_3]$, $\eta^5 \rightarrow \eta^1$ ring slippage is observed in the presence of PMe_3 and PBu_3, at room temperature, or with bipy at 54°C, but the kinetically required η^3 intermediate could not be detected chemically or spectroscopically (Eq. (3) [4]).

In view of these results and given the facility of many of the above-reported ring slippages, it is rather unexpected that the weakly coordinating labile NCMe is capable of inducing an $\eta^5 \rightarrow \eta^3$ haptotropic rearrangement, **1a** → **4a**, whereas the strong donor PMe_3 is not. As shown by Merola et al. [3] and Casey and O'Connor [4], bulky donors do not favour ring slippages which are otherwise facile with PMe_3. However, in our reactions, no important steric problems hindering ligand addition to any of the complexes **1b**, **1f–1h** are apparent. For instance, one would expect ready addition of NCMe to derivative $[(\eta^5\text{-Ind})M(CO)_2bipy]^+$ (**1b**), where there are two N-donor ligands and bipy does not create steric problems if coordinated to the equatorial plane of the putative final octahedral product, $[Mo(\eta^3\text{-Ind})(CO)_2\text{-(NCMe)(bipy)}]BF_4$. In fact, a crystal structure of $[Mo(\eta^3\text{-}C_3H_5)(CO)_2\text{-(NCMe)(bipy)}]BF_4$ has the *fac*-{(NCMe)bipy} ligand arrangement and does not reveal any important intramolecular steric strain [24]. Clearly, ligands such as $CH(pz)_3$, $[HB(pz)_3]^-$ and Me_3tacn all possess a much larger steric bulk than the combined *fac*-{(NCMe)bipy} ligand arrangement. Nevertheless, they are capable of inducing or stabilizing indenyl slippage in the present system, whereas the *fac*-{(NCMe)bipy} ligand arrangement is not.

One may argue that ring slippage promoted by $CH(pz)_3$, $[HB(pz)_3]^-$ or Me_3tacn is favoured by the coordination geometry and the chelate effect of the tridentate ligands which overcome electronic barriers present in the *fac*-{(NCMe)bipy} ligand set. However, the reasons for the facile addition of NCMe or DMF to both **1a** and **2** must be almost entirely electronic as steric problems are obviously absent. The identification of these "electronic" factors or conditions should be important for understanding the reactivity enhancement of indenyl complexes and the "indenyl effect" and an independent MO study of these and related problems is under way.

3. Conclusions

Stable octahedral complexes of molybdenum and tungsten bearing the trihapto-indenyl ligand, $[(\eta^3\text{-Ind})M(CO)_2L_2L']^+$, are easily accessible from four-legged piano-stool precursors, $[(\eta^5\text{-Ind})M(CO)_2L_2]^+$, by addition of L′. This otherwise rare addition or ring-slippage reaction is facile for a series of *N*-donor ($L_2L' = (NCMe)_3$, $CH(pz)_3$, $[HB(pz)_3]^-$ or Me_3tacn) and DMF but is not observed for the corresponding

complexes with L_2 = bipy, $(PMe_3)_2$, $(P(OMe)_3)_2$, dppe or triphos. The reasons for this unexpected behaviour seem to be essentially electronic in character and prompt theoretical and experimental studies with other ligands (N, P, S and O).

4. Experimental details

All preparations and manipulations were done with standard Schlenk techniques under argon. Solvents were dried by standard procedures (tetrahydrofuran and Et_2O over Na–benzophenone ketyl; CH_2Cl_2, NCMe and NCEt over CaH_2) distilled under argon and kept over 4 Å molecular sieves (3 Å for NCMe).

Microanalyses were performed at the Instituto de Tecnologia Química e Biológica. NMR spectra were measured on a Bruker CXP 300, ^1H and ^{13}C chemical shifts are reported on the scale relative to $SiMe_4$ ($\delta = 0.0$ ppm) and the ^{31}P spectra are given relative to TMP–solvent [25]. IR spectra were obtained using a Unicam Mattson Model 7000 Fourier transform spectrometer. $[IndMo(NCMe)_2(CO)_2]BF_4$ (**1a**) [6a] and $[IndW(NCMe)_2(CO)_2]BF_4$ (**2**) [5] were prepared as published.

4.1. Preparation of $[IndMobipy(CO)_2]BF_4$ (1b)

A solution of $[IndMo(\eta^3\text{-}C_3H_5)(CO)_2]$ (0.22 g, 0.71 mmol) in CH_2Cl_2 (15 ml) was treated with $HBF_4 \cdot Et_2O$ (1 equivalent). After 10 min 2,2'-bipyridyl was added (0.13 g, 0.85 mmol) and the mixture left for 1 h. After concentration to about 5 ml and addition of ether, a pink–red complex precipitated. The mixture was filtered and the residue recrystallized from CH_2Cl_2–Et_2O (yield, 98%). Anal. Found: C, 49.38; H, 3.05; N, 5.42. for $C_{21}H_{15}BF_4MoN_2O_2$ Calc.: C, 49.45; H, 2.96; N, 5.46%. Selected IR (KBr): ν(CO) 1975, 1958, 1901, 1874 vs cm^{-1} ^1H NMR (NCMe-d_3, 300MHz): δ 9.36 (d, 2H, bipy); 8.30 (d, 2H, bipy); 8.07 (t, 2H, bipy); 7.57 (t, 2H, bipy); 6.95 (m, 2H, H^{5-8}); 6.66 (m, 2H, H^{5-8}); 6.47 (d, 2H, $H^{1/3}$); 5.47 (t, 1H, H^2) ppm.

4.2. Preparation of $[IndMo(\eta^2\text{-}tpm)(CO)_2]BF_4$ (1c)

A solution of $[IndMo(NCMe)_2(CO)_2]BF_4$ (0.32 g, 0.73 mmol) in CH_2Cl_2 (20 ml) was treated with trispyrazolylmethane (0.16 g, 0.75 mmol) for 30 min. The pale-pink powder was filtered off and washed with ether (yield, 90%). Anal. Found: C, 44.53; H, 2.96; N, 14.62. $C_{21}H_{17}BF_4MoN_6O_2$ Calc.: C, 44.39; H, 2.99; N, 14.78%. Selected IR (KBr): ν(CO) 1958, 1883 vs cm^{-1}.

4.3. Preparation of $[IndMo(DMF)_2(CO)_2]BF_4$ (1d)

A solution of $[IndMo(\eta^3\text{-}C_3H_5)(CO)_2]$ (0.10 g, 0.32 mmol) in CH_2Cl_2 (20 ml) was treated with $HBF_4 \cdot Et_2O$ (1 equivalent). After 10 min an excess of DMF (2 ml) was added and the mixture left for 1 h. The solvent was evaporated and the residue recrystallized from CH_2Cl_2–Et_2O (yield, 88%). Selected IR (Nujol): ν(CO) 1962, 1865 vs, ν(C=O) 1657 vs cm^{-1}. ^1H NMR (CH_2Cl_2-d_2 300 MHz): δ 8.04 (s, CH); 7.47 (m, 2H, H^{5-8}); 7.39 (m, 2H, H^{5-8}); 6.15 (d, 2H, $H^{1/3}$); 4.98 (t, 1H, H^2); 3.01 (s, 6H, CH_3); 2.72 (s, 6H, CH_3) ppm.

4.4. Preparation of $[IndMo(en)(CO)_2]BF_4$ (1e)

A solution of $[IndMo(\eta^3\text{-}C_3H_5)(CO)_2]$ (0.20 g, 0.65 mmol) in CH_2Cl_2 (20 ml) was treated with $HBF_4 \cdot Et_2O$ (1 equivalent). After 10 min, an excess of H_2NCH_2-CH_2NH_2 was added and the reaction left for 1 h. After concentration to about 5 ml and addition of ether, the orange precipitate was filtered off and washed with ether (yield, 92%). Anal. Found: C, 37.58; H, 3.59; N, 6.51. $C_{13}H_{15}BF_4MoO_2N_2$ Calc.: C, 37.71; H, 3.65 N, 6.77%. Selected IR. (KBr), ν(CO) 1969, 1854 vs cm^{-1}. ^1H NMR (Me_2CO-d_6, 300 MHz): δ 7.84 (m, 2H, H^{5-8}); 7.51 (m, 2H, H^{5-8}); 6.23 (d, 2H, $H^{1/3}$); 5.18 (t, 1H, H^2); 5.41 (br, 2H, NH_2); 3.08 (br, 2H, NH_2); 2.33 (m, 2H, CH_2); 1.69 (m, 2H, CH_2) ppm.

4.5. Preparation of $[IndMo\{P(OMe)_3\}_2(CO)_2]BF_4$ (1f)

A solution of $[IndMo(\eta^3\text{-}C_3H_5)(CO)_2]$ (0.20 g, 0.65 mmol) in CH_2Cl_2 (15 ml) was treated with $HBF_4 \cdot Et_2O$ (1 equivalent). After 10 min, $P(OMe)_3$ was added (0.15 ml, 1.3 mmol) and the mixture left for 1 h. After concentration to about 8 ml and addition of ether, a microcrystalline yellow precipitate was filtered off and washed with ether (yield, 95%). Anal. Found: C, 34.07; H, 4.18. $C_{17}H_{25}BF_4MoO_8P_2$ Calc.: C, 33.91; H, 4.19%. Selected IR (KBr): ν(CO) 1991, 1906 vs cm^{-1}. ^1H NMR (NCMe-d_3, 300 MHz): δ 7.59 (m, 2H, H^{5-8}); 7.30 (m, 2H, H^{5-8}); 6.07 (d, 2H, $H^{1/3}$); 5.60 (t, 1H, H^2); 3.75 (d, 18H, $J_{PH} = 11.2$ Hz, OCH_3) ppm. ^{31}P (NCMe-d_3, 121.49 MHz, 25°C): δ −58.93 (br, $P(OMe)_3$) ppm.

4.6. Preparation of $[IndMo(PMe_3)_2(CO)_2]BF_4$ (1g)

A solution of $[IndMo(\eta^3\text{-}C_3H_5)(CO)_2]$ (0.20 g, 0.65 mmol) in CH_2Cl_2 (15 ml) was treated with $HBF_4 \cdot Et_2O$ (1 equivalent). After 10 min, PMe_3 was added (0.13 ml, 1.3 mmol) and the mixture left for 1 h. After concentration to about 8 ml and addition of ether, a microcrystalline pale-yellow precipitate was filtered off and washed with ether (yield, 95%). Anal. Found: C, 40.13; H, 5.00, $C_{17}H_{25}BF_4MoO_2P_2$ Calc.: C, 40.35; H, 4.98%. Selected IR (KBr): ν(CO) 1958, 1877 vs cm^{-1}. ^1H NMR (NCMe-d_3, 300 MHz): δ 7.66 (m, 2H, H^{5-8}); 7.28 (m, 2H, H^{5-8}); 5.85 (d, 2H, $H^{1/3}$); 5.54 (t, 1H, H^2); 1.66 (d, 18H, $J_{PH} = 8.7$ Hz, CH_3) ppm. ^{31}P

(NCMe-d_3, 121.49 MHz, 25°C): δ 13.10 (s, PMe_3) ppm.

4.7. Preparation of [IndMo(dppe)(CO)$_2$]BF$_4$ (1h)

A solution of [IndMo(η^3-C_3H_5)(CO)$_2$] (0.20 g, 0.65 mmol) in CH_2Cl_2 (15 ml) was treated with $HBF_4 \cdot Et_2O$ (1 equivalent). After 10 min, 1,2 bis(diphenylphosphino)ethane was added (0.30 g, 0.75 mmol) and the reaction mixture left for 1 h. After concentration to half the initial volume and addition of ether, the yellow precipitate was filtered off and washed with ether. It was then recrystallized from CH_2Cl_2–Et_2O (yield, 94%). Anal. Found: C, 59.00; H, 4.00. $C_{37}H_{31}BF_4MoO_2P_2$ Calc.: C, 59.07; H, 4.15%. Selected IR (KBr): ν(CO) 1973, 1904 vs cm^{-1}. ^{1}H NMR (NCMe-d_3, 300 MHz): δ 7.66–7.32 (m, 20H, Ph); 7.08 (m, 2H, H^{5-8}); 6.01 (m, 2H, H^{5-8}); 5.59 (d, 2H, $H^{1/3}$); 5.28 (t, 1H, H^2); 2.64 (br, 4H, CH_2) ppm. ^{31}P NMR (NCMe-d_3, 121.49 MHz, 25°C): δ 35.86 (br, dppe); 15.08 (br, dppe) ppm.

4.8. Preparation of [IndMo(triphos)(CO)$_2$]BF$_4$ (1i)

A solution of [IndMo(η^3-C_3H_5)(CO)$_2$] (0.20 g, 0.65 mmol) in CH_2Cl_2 (15 ml) was treated with HBF_4–Et_2O (1 equivalent). After 10 min, triphos was added (0.40 g, 0.65 mmol) and the reaction mixture left for 2 h. After concentration to half the initial volume and addition of ether, the yellow precipitate was filtered off and washed with ether (yield, 94%). Selected IR (KBr): ν(CO) 1965, 1909 vs cm^{-1}. ^{1}H NMR (Me_2CO-d_6, 300 MHz): δ 7.85–7.10 (m, 30H, Ph); 7.06 (m, 2H, H^{5-8}); 6.58 (m, 2H, H^{5-8}); 5.71 (t, 1H, H^2); 5.36 (d, 2H, $H^{1/3}$); 2.77 (m, 4H, CH_2); 2.55 (m, 2H, CH_2); 1.16 (m, 3H, CH_3) ppm.

4.9. Preparation of [CpMo{η^2-HC(pz)$_3$}(CO)$_2$]BF$_4$ (3)

A solution of [CpMo(η^3-C_3H_5)(CO)$_2$] (0.25 g, 0.97 mmol) in CH_2Cl_2 (20 ml) was treated with HBF_4–Et_2O (1 equivalent). After 10 min a slight excess of trispyrazolylmethane (0.21 g, 1.0 mmol) was added and stirring continued for 1 h. The reaction mixture was then concentrated and Et_2O added to precipitate an orange product which was further recrystallized from CH_2Cl_2–Et_2O (yield, 92%). Anal. Found: C, 39.25; H, 2.81; N, 16.26. $C_{17}H_{15}BF_4MoN_6O_2$ Calc.: C, 39.41; H, 2.92; N, 16.22%. Selected IR (KBr): ν(CO) 1983, 1912 vs cm^{-1}. ^{1}H NMR (NCMe-d_3, 300 MHz, room temperature): δ 8.51 (s, 1H, CH), 8.47 (dd, 2H, H^3), 8.04 (dt, 2H, H^5), 7.50 (d, 1H, H^5), 6.77 (dd, 2H, H^4), 6.60 (d, 1H, H^3), 6.36 (dd, 1H, H^4), 5.80 (s, 5H, Cp) ppm. ^{13}C NMR (NCMe-d_3, 75 MHz, room temperature); δ 253.29, CO; 154.62, 2C^3; 142.71, C^3; 141.10, 2C^5; 129.59, C^5; 110.87, 2C^4; 108.89, C^4; 99.32, Cp; 80.50, CH ppm.

4.10. Preparation of [IndMo(NCMe)$_3$(CO)$_2$]BF$_4$ (4a)

A solution of [IndMo(NCMe)$_2$(CO)$_2$]BF_4 (0.22 g, 0.50 mmol) in NCMe (20 ml) was warmed to 45°C for 30 min. The resulting dark-red solution was concentrated and addition of Et_2O gave the crystalline product, which was further recrystallized from NCMe–Et_2O (yield, 98%). Anal. Found: C, 42.75; H, 3.30; N, 8.75. $C_{17}H_{16}BF_4MoN_3O_2$ Calc.: C, 42.80; H, 3.38; N, 8.81%. Selected IR (Nujol): ν(N=C) 2317, 2287 w; ν(CO) 1962, 1890 vs cm^{-1}. Selected IR (KBr): ν(CO) 1964, 1869 vs cm^{-1}. ^{1}H NMR (NCMe-d_3, 300 MHz, −40°C): δ 7.20 (t, 1H, H^2), 6.47–6.37 (m, 4H, H^{5-8}), 5.10 (d, 2H, $H^{1/3}$), 1.95 (s, 9H, CH_3) ppm. ^{13}C NMR (NCMe-d_3, 75 MHz, −40°C): δ 221.50, CO; 146.73, C$^{4/9}$; 125.03, C$^{5/8}$; 118.20, C$^{6/7}$; 118.16 (s, $NCCD_3$ and NCMe); 98.72, C^2; 75.40, C$^{1/3}$, 1.81–0.19 (m, $NCCD_3$ and NCMe) ppm.

4.11. Preparation of [(η^3-Ind)Mo{η^3-HC(pz)$_3$}(CO)$_2$]BF$_4$ (4b)

A solution of [IndMo(η^2-tpm)(CO)$_2$]BF_4 (0.20 g, 0.35 mmol) in NCMe (20 ml) was warmed to 45°C for 2 h. The solution was concentrated and addition of Et_2O gave an orange product which was further recrystallized from NCMe–Et_2O (−30°C) (yield, 98%). Anal. Found: C, 44.28; H, 3.00; N, 14.70. $C_{21}H_{17}BF_4MoN_6O_2$ Calc.: C, 44.39; H, 2.99; N, 14.78%. Selected IR (KBr) ν(CO) 1946, 1867 vs cm^{-1}. ^{1}H NMR (NCME-d_3, 300 MHz, room temperature): δ 9.11 (d 1H, H_5), 8.55 (s, 1H, CH), 8.14 (d, 1H, H_3), 8.12 (d, 2H, H_3), 8.05 (d, 2H, H_5), 6.90 (t, 1H, H^2), 6.72–6.69 (m, 3H, $2H^{5-8} + H_4$), 6.59–6.51 (m, 4H, $2H^{5-8} + 2H_4$) 5.55 (d, 2H, $H^{1/3}$) ppm. ^{13}C NMR (NCMe-d_3, 75 MHz, room temperature): 226.50, CO; 153.70, C_3; 147.80, C$^{4/9}$; 146.99, $2C_3$; 135.74, $2C_5$; 134.90, C_5; 125.63, C$^{5/8}$; 119.01, C$^{6/7}$; 110.67, C_4; 109.29, $2C_4$; 99.76, C^2; 76.07, C$^{1/3}$; 75.69, CH ppm.

4.12. Preparation of [(η^3-Ind)Mo{η^3-HB(pz)$_3$}(CO)$_2$] (4c)

A solution of [IndMo(NCMe)$_2$(CO)$_2$][BF_4] (0.22 g, 0.50 mmol) in CH_2Cl_2 (20 ml) was treated with K[HB(pz)$_3$] (0.13 g, 0.52 mmol). After 2 h the solvent was removed under vacuum and the residue extracted with hexane. Ether was added and after concentration and evaporation the compound separated as brick-red microcrystals. Further recrystallization was from hexane–Et_2O (yield, 86%). Anal. Found: C, 50.10; H, 3.55; N, 17.68. $C_{20}H_{17}BMoN_6O_2$ Calc.: C, 50.03; H, 3.57; N, 17.50%. Selected IR (KBr): ν(BH) 2475; ν(CO) 1939, 1848 vs cm^{-1}. ^{1}H NMR (NCMe-d_3, 300 MHz, room temperature): δ 8.86 (d, 1H, H_5), 7.81 (d, 2H, H_5), 7.65 (d, 2H, H_3), 7.64 (d, 1H, H_3), 6.63 (t,

1H, H^2), 6.70–6.67 (m, 2H, H^{5-8}), 6.52–6.49 (m, 2H, H^{5-8}), 6.44 (t, 1H, H_4), 6.25 (d, 2H, H_4), 5.40 (d, 2H, $H^{1/3}$) ppm. ^{13}C NMR (NCMe-d_3, 75 MHz, room temperature): δ 229.88, CO; 150.46, C_3; 148.56, $C^{4/9}$; 143.81, $2C_3$; 137.32, $2C_5$; 136.08, C_5; 124.83, $C^{5/8}$; 118.50, $C^{6/7}$; 108.35, C_4; 106.77, $2C_4$; 99.59, C^2; 75.05, $C^{1/3}$ ppm. Mass spectroscopy m/z 424 ($M^+ - 2CO$); 308 ($M^+ - C_9H_7$).

4.13. Preparation of $[(\eta^3\text{-Ind})Mo\{\eta^3\text{-}Me_3tacn\}(CO)_2]BF_4$ (4d)

A solution of $[IndMo(NCMe)_2(CO)_2][BF_4]$ (0.25 g, 0.57 mmol) in CH_2Cl_2 (20 ml) was treated with an excess of 1,4,7-trimethyltriazocyclononan (0.40 ml). After 1 h the resulting dark-red solution was concentrated and addition of Et_2O gave the product, which was further recrystallized from NCMe–Et_2O (−30°C) (yield, 85%). Anal. Found: C, 45.59; H, 5.20; N, 8.01. $C_{20}H_{28}BF_4MoN_3O_2$ Calc.: C, 45.74; H, 5.37; N, 8.00%. Selected IR (KBr): ν(CO) 1937, 1852 vs cm^{-1}. (NCMe-d_3, 300 MHz, room temperature): δ 6.94 (t, 1H, H^2), 6.60 (m, 2H, H^{5-8}); 6.47 (m, 2H, H^{5-8}), 4.78 (d, 2H, $H^{1/3}$), 3.99 (s, 3H, CH_3), 3.05 (m, 6H, CH_2), 2,72 (s, 6H, CH_3), 2.69 (m, 6H, CH_2) ppm. ^{13}C NMR (CH_2Cl_2-d_2, 75 MHz, room temperature): δ 227.31, CO; 147.03, $C^{4/9}$; 125.56, $C^{5/8}$; 118.09, $C^{6/7}$; 93.80, C^2; 73.43, $C^{1/3}$; 59.53, 59.18, 57.65, CH_2 and CH_3 ppm.

Table 6
Summary of crystal data and details of intensity collection for **5**

Crystal data	
Formula	$C_{17}H_{16}N_3O_2W$–BF_4
Formula weight	530.0
Crystal system	Orthorhombic
Space group	$Cmc2_1$ (No. 36)
a (pm)	1048.8(1)
b (pm)	1350.4(2)
c (pm)	2765.3(4)
Cell volume (10^6 pm^3)	3916.5(9)
Z; d_{calc} g cm^{-3}	4; 1.916
F(000)	2160
Crystal size (mm)	0.38 × 0.25 × 0.386
Crystal colour and habit	Red–brown prisms
Data collection and data reduction	
Diffractometer	Enraf–Nonius CAD4
Radiation	Mo Kα (λ = 71.073 pm)
Temperature (K)	193 ± 3
Scan type	ω scan
Scan range (°)	1.20 + 0.25 tan Θ
Scan time (s)	Variable; maximum 90
2Θ limits, (°); octants	2.0–50.0; $+h$, $+k$, $\pm l$
Number of reflections collected	3811
Number of reflections for ψ scan	9
m (Mo Kα) (cm^{-1})	59.5
Transmission factor: maximum; minimum	0.775 : 1.000
Crystal decay (%)	No
Extinction parameter	2.7×10^{-7}
Solution and refinement	
Number of independent data	3615
Number of observed data	3615 ($I > 0.00$)
Number of refined parameters	370
Weighting scheme: $w^{-1} = \sigma^2(F_o^2) + aP^2 + bP$	$P = (F_o^2 + 2F_c^2)/3$ $a = 0.0202$; $b = 19.32$
R indices (all data)	
R_1 [a]	0.018
wR_2 [b]	0.045
Flack parameter	0.05(1)
Goodness of fit [c]	1.099
Peak final difference map: maximum; minimum (electrons $Å^{-3}$)	0.51; 0.52
Maximum shift/error	< 0.001

[a] $R_1 = \Sigma \| F_o | - | F_c \| / \Sigma F_o$.
[b] $wR_2 = [\Sigma w(F_o^2 - F_c^2)^2 / \Sigma w(F_o)^2]^{1/2}$.
[c] Goodness of fit = $[\Sigma w(F_o^2 - F_c^2)^2 / (N_O\text{-}N_V)]^{1/2}$.

4.14. Preparation of [IndMo(DMF)$_3$(CO)$_2$]BF$_4$ (4e)

A solution of [IndMo(η^3-C_3H_5)(CO)$_2$] (0.10 g, 0.32 mmol) in CH_2Cl_2 (20 ml) was treated with $HBF_4 \cdot Et_2O$ (1 equivalent). After 10 min an excess of DMF (5 ml) was added and the reaction mixture left for 1 h. The solvent was evaporated and the residue recrystallized from DMF–Et_2O (yield, 91%). Selected IR (Nujol): ν(CO) 1939, 1848 vs, ν(C=O) 1649 cm^{-1}. ^{1}H NMR (DMF-d_7, 300 MHz, room temperature): δ 8.02 (s, CH); 6.99 (t, 1H, H^2); 6.47–6.39 (m, 4H, H$^{5-8}$); 5.08 (d, 2H, H$^{1/3}$); 2.95 (s, CH_3); 2.78 (s, CH_3) ppm. ^{13}C NMR (DMF-d_7, 75 MHz, room temperature): δ 229.94, CO; 162.8 (s, DMF); 146.73 C$^{4/9}$; 123.70, C$^{5/8}$; 117.20, C$^{6/7}$; 101.30, C^2; 74.53, C$^{1/3}$; 35.70 (s, DMF); 30.6 (s, DMF) ppm.

4.15. Preparation of [IndW(CO)$_2$(NCMe)$_3$]BF$_4$ (5)

A solution of [IndW(CO)$_2$(NCMe)$_2$]BF$_4$ (0.28 g; 0.49 mmol) in NCMe (20 ml) was warmed to 45°C for 30 min. The resulting dark-red solution was concentrated and addition of Et_2O gave the crystalline product which was further recrystallized from NCMe–Et_2O (yield, 96%), Anal. Found: C, 36.08; H, 2.99; N, 7.38. $C_{17}H_{16}BF_4O_2N_3W$ Calc.: C, 36.14; H, 2,85; N, 7.44%. Selected IR (Nujol): ν(N=C) 2318, 2288 w; ν(CO) 1952, 1881 vs cm^{-1}. Selected IR (KBr): ν(CO) 1948,

Table 7
Final coordinates and equivalent isotropic thermal parameters of the non-hydrogen atoms for [η^3-IndW(CO)$_2$(NCMe)$_3$]BF$_4$ (5)

Atom	x	y	z	U_{eq} (Å^2)
W(1)	0	0.09025(2)	0.22198(1)	0.0244(1)
O(1)	0.1894(4)	0.0167(3)	0.3013(1)	0.043(1)
N(1)	0	0.2368(5)	0.2526(2)	0.030(2)
N(2)	0.1391(5)	0.1614(3)	0.1739(2)	0.034(1)
C(1)	0.1229(5)	0.0458(4)	0.2711(2)	0.030(2)
C(2)	0	0.3161(6)	0.2666(3)	0.029(2)
C(3)	0	0.4182(7)	0.2851(4)	0.047(3)
C(4)	0.2089(6)	0.1944(4)	0.1471(2)	0.034(2)
C(5)	0.2997(8)	0.2359(6)	0.1138(3)	0.054(2)
C(6)	0	−0.0210(6)	0.1660(3)	0.032(2)
C(7)	0.1089(6)	−0.0536(4)	0.1929(2)	0.033(2)
C(8)	0.0677(4)	−0.1386(3)	0.2222(2)	0.029(1)
C(9)	0.1351(6)	−0.2105(4)	0.2466(2)	0.037(2)
C(10)	0.0648(7)	−0.2865(4)	0.2691(2)	0.038(2)
W(2)	0	0.119166(2)	0.43481(1)	0.0251(1)
O(2)	0.1903(4)	0.2638(3)	0.3556(1)	0.043(1)
N(3)	0	0.0451(5)	0.4037(2)	0.032(2)
N(4)	0.1389(5)	0.1207(4)	0.4827(2)	0.039(1)
C(11)	0.1228(5)	0.2364(4)	0.3855(2)	0.031(2)
C(12)	0	−0.0326(6)	0.3899(3)	0.033(2)
C(13)	0	−0.1329(9)	0.3721(4)	0.048(3)
C(14)	0.2075(8)	0.0833(5)	0.5079(3)	0.053(2)
C(15)	0.2960(14)	0.0359(9)	0.5418(4)	0.103(5)
C(16)	0	0.3054(5)	0.4910(3)	0.032(3)
C(17)	0.1079(6)	0.3342(4)	0.4634(2)	0.031(2)
C(18)	0.0675(5)	0.4196(3)	0.4335(2)	0.038(1)
C(19)	0.1339(6)	0.4931(4)	0.4097(2)	0.036(2)
C(20)	0.0654(7)	0.5688(5)	0.3864(2)	0.043(2)
F(1)	0	0.5446(5)	0.1076(2)	0.072(3)
F(2)	0.0863(15)	0.4037(8)	0.1378(5)	0.108(6) [a]
F(3)	0.1024(11)	0.4544(16)	0.1632(7)	0.144(9) [a]
F(4)	0.0731(16)	0.5353(11)	0.1830(4)	0.127(7) [a]
B(1)	0	0.4835(11)	0.1486(4)	0.064(4)
F(5)	0	0.0971(9)	0.0577(3)	0.187(8)
F(6)	0.0709(15)	0.1278(10)	−0.0163(4)	0.103(5) [a]
F(7)	0.0723(20)	0.2459(12)	0.0361(8)	0.160(10) [a]
F(8)	0.1048(13)	0.1912(21)	0.0110(10)	0.206(17) [a]
B(2)	0	0.1642(11)	0.0235(4)	0.064(5)

U_{eq} is defined as a third of the trace of the orthogonalized U_{ij} tensor.
[a] Atom sites have a population of 0.500.

1874 vs cm^{-1}. ^1H NMR (NCMe-d_3, 300 MHz, room temperature): δ 6.55–6.48 (m, 5H, H^{5-8} and H^2); 5.02 (d, 2H, $H^{1/3}$); 1.96 (s, CH_3) ppm. ^{13}C NMR (NCMe-d_3; 75 MHz, room temperature): δ 213.93, CO; 149.23, $C^{4/9}$; 125.03, $C^{5/8}$; 119.04, $C^{6/7}$; 118.28 (s, $NCCD_3$ and NCMe); 91.72; C^2; 66.20, $C^{1/3}$; 2.09–0.48 (m, $NCCD_3$ and NCMe) ppm.

4.16. X-ray structure determination of 5

Details of data collection parameters, structure solution and refinement for **5** are presented in Table 6, and the final positional parameters in Table 7. A red–brown prism, coated with silicone grease in a glass capillary, was mounted on a CAD4 diffractometer equipped with a graphite monochromator. For determination of accurate cell dimensions the positional parameters of 25 reflection (each centred in four orientations; $\theta > 20.0°$) were refined by full-matrix least-squares methods. During data collection, the intensities of three standard reflections where monitored and showed no decay. Corrections for Lorentz–polarization effects, absorption and extinction were applied. From the original data set 196 reflections (20 with $I < 0.01$; 176 systematically absent) were rejected. The structure was solved by the heavy-atom method and subsequent difference Fourier synthesis and refined by full-matrix least-squares methods, with anisotropic thermal parameters for the non-hydrogen atoms. All H atoms were identified in difference maps and were refined with isotropic thermal parameters. Both of two BF_4^- anions were found disordered in two positions. Scattering factors for neutral atoms and values for anomalous dispersion were taken from reference 26 and programs for solution and refinement [27] were run on a Micro VAX 3100.

Further details of the crystal structure investigation are available on request from the Fachinformationszentrum Karlsruhe, D-76344 Eggenstein-Leopoldshafen, on quoting the depository number CSD-401921, the names of the authors and the journal citation, or from one of the authors E.H.

Acknowledgments

This work was financially supported by the Junta Nacional de Investigação Científica e Tecnológica (JNICT). ISG thanks JNICT for grants. We thank Professor W.A. Herrmann, Technische Universität Munich, for providing analytical facilities and mass spectra.

References and note

[1] M.E. Rerek, L.-N. Ji and F. Basolo, *J. Chem. Soc., Chem. Commun.*, (1983) 1208–1209.

[2] (a) J.M. O'Connor and C.P. Casey, *Chem. Rev., 87* (1987) 307–318; (b) A.K. Kakkar, S.F. Jones, N.J. Taylor, S. Collins and T.B. Marder, *J. Chem. Soc., Chem. Commun.*, (1989) 1454–1456.

[3] J.S. Merola, R.T. Kacmarcyk and D. Van Engen, *J. Am. Chem. Soc., 108* (1986) 329–331.

[4] C.P. Casey and J.M. O'Connor, *Organometallics, 4* (1985) 384–388.

[5] I.S. Gonçalves and C.C. Romão, *J. Organomet. Chem., 486* (1995) 155–161.

[6] (a) J.A. Ascenso, C.G. de Azevedo, I.S. Gonçalves, E. Herdtweck, D. Moreno, M. Pessanha and C.C. Romão, *Organometallics*, in press; (b) J.A. Ascenso, C.G. de Azevedo, I.S. Gonçalves, E. Herdtweck, D. Moreno, C.C. Romão and J. Zühlke, *Organometallics, 13* (1994) 429–431.

[7] J. Markham, K. Menard and A. Cutler, *Inorg. Chem., 24* (1985) 1581–1587.

[8] (a) M. Botrill and M. Green, *J. Chem. Soc., Dalton Trans.*, (1977) 2365; (b) M. Green, S. Greenfield and M. Kersting, *J. Chem. Soc., Chem. Commun.*, (1985) 18–20.

[9] D.J. Norris, J.F. Corrigan, Y. Sun, N.J. Taylor and S. Collins, *Can. J. Chem., 71* (1993) 1029.

[10] A leading discussion of NMR spectra of $HC(pz)_3$ complexes may be found in: (a) M.A. Esteruelas, L.A. Oro, M.C. Apreda, C. Foces-Foces, F.H. Cano, R.M. Claramunt, C. Lopez, J. Elguero and M. Begtrup, *J. Organomet. Chem., 344* (1988) 93; (b) M.A. Esteruelas, L.A. Oro, R.M. Claramunt, C. Lopez, J.L. Lavandera and J. Elguero, *J. Organomet. Chem., 366* (1989) 245.

[11] Trofimenko, S., *J. Am. Chem. Soc., 92* (1970) 5118.

[12] A.N. Nesmeyanov, N.A. Ustynyuk, L.G. Makarova, V.G. Andrianov, Yu.T. Struchkov, S. Andrae, Yu.A. Ustynyuk and S.G. Malyugina, *J. Organomet. Chem., 159* (1978) 189–199.

[13] J.W. Faller, R.H. Crabtree and A. Habib, *Organometallics, 4* (1985) 929.

[14] T.B. Marder, J.C. Calabrese, D.C. Roe and T.H. Tulip, *Organometallics, 6* (1987) 2012; (b) R.T. Baker and T.H. Tulip, *Organometallics, 5* (1986) 839.

[15] M.B. Honan, J.L. Atwood, I. Bernal, W.A. Herrmann, *J. Organomet. Chem., 179* (1979) 403.

[16] J.R. Bocarsly, C. Floriani, A. Chiesi-Villa and C. Guastini, *Inorg. Chem., 26* (1987) 1871.

[17] R.M. Kowalewski, A.L. Rheingold, W.C. Trogler and F. Basolo, *J. Am. Chem. Soc., 108* (1986) 2460–2461.

[18] G. Huttner, H.H. Brinzinger, L.G. Bell, P. Friedrich, V. Benjenke and D. Neugebauer, *J. Organomet. Chem., 145* (1978) 329.

[19] F. Dawans, J. Dewailly, J. Meunier-Piret and P. Piret, *J. Organomet. Chem., 76* (1974) 53.

[20] A.J. Graham, D. Akrigg and B. Sheldrick, *Cryst. Struct. Commun., 6* (1977) 253.

[21] M. Boyer, J.-C. Daran and Y. Jeannin, *J. Organomet. Chem., 190* (1980) 177.

[22] C.A. Gamelas, I.S. Gonçalves and C.C. Romão, unpublished results, 1995.

[23] T.C. Forschner, A.R. Cutler and R.K. Kullnig, *Organometallics, 6* (1987) 889.

[24] A.M. Galvão, *Ph.D. Dissertation*, Technical University of Lisbon, 1993.

[25] L.A. Combs-Walker and C.L. Hill, *Inorg. Chem., 30* (1991) 4016–4026.

[26] A.J.C. Wilson (ed.), *International Tables for Crystallography*, Vol. C, Kluwer, Dordrecht 1992, Table 6.1.1.4 (pp. 500–502), Table 4.2.6.8 (pp. 219–222) and Table 4.2.4.2 (pp. 193–199).

[27] PLATON-92, PLUTON-92, SCHAKAL, SDP, SHELXL-93 and STRUX-V.